

Cite this article as: Zheng Wei, Han Junzhao, Duan Xing, et al. Mechanical Properties of Al_{0.1}CoCrFeNi High Entropy Alloy Based on Molecular Dynamics Study[J]. Rare Metal Materials and Engineering, 2022, 51(09): 3230-3235.

ARTICLE

Mechanical Properties of Al_{0.1}CoCrFeNi High Entropy Alloy Based on Molecular Dynamics Study

Zheng Wei¹, Han Junzhao¹, Duan Xing², Chen Wenhua¹

¹ National and Local Joint Engineering Research Center of Reliability Analysis and Testing for Mechanical and Electrical Products, Zhejiang Sci-Tech University, Hangzhou 310018, China; ² College of Materials and Environmental Engineering, Hangzhou Dianzi University, Hangzhou 310018, China

Abstract: The microstructure and mechanical properties of Al_{0.1}CoCrFeNi single crystal high entropy alloy (HEA) under axial tensile loading at room temperature (300 K) were investigated by molecular dynamics method. The tensile properties of the single crystal HEA were analyzed by changing the simulated strain rate and temperature. The microstructure and tensile properties of the single crystal HEA with small surface cracks were studied by simulating tensile experiments at room temperature. Results demonstrate that the tensile strength is increased with increasing the strain rate in a certain range; the Young's modulus and tensile strength are increased with decreasing the temperature at strain rate of 10¹⁰ s⁻¹. The single crystal HEA with small through cracks on surface presents a necking phenomenon after stretching for a period, and the stress concentration occurs at the crack tip along with the rapid development of a large number of slip dislocations, resulting in the rapid fracture.

Key words: high entropy alloy; molecular dynamics; tensile properties; crack

The high entropy alloy (HEA) has excellent properties^[1], such as ultra-high strength, good plasticity, and damage tolerance, and it can easily form single-phase solid solution, which attracts much attention in recent years^[2,3]. Particularly, four core effects of HEAs have been widely investigated and applied: high entropy, lattice distortion, sluggish diffusion, and cocktail effect^[4].

HEAs can be classified by the element proportion into equimolar and non-equimolar HEAs. In addition, HEAs can also be distinguished through the crystal structure of single-phase solid solution of HEAs, such as CoCrMnNi^[5] and Al_{0.3}CoCrFeNi^[6] alloys with face-centered cubic (fcc) structure, MoNbTaVW^[7] alloy with body-centered cubic (bcc) structure, and Al₅Sc₂₀Hf₂₅Ti₂₅Zr₂₅^[8] alloy with hexagonal close-packed (hcp) structure.

Rogal et al^[9] prepared four types of Al-Co-Cr-Fe and Al-Co-Cr-Fe-Ni HEAs with different components by mechanical alloying and spark plasma sintering consolidation. The matrix and grains of the alloys have fcc structure and the variation of

mechanical properties corresponds to the crystal structure change. It is demonstrated that the nickel addition leads to the formation of plastic fcc phase, which causes the decrease in strength with increasing the plasticity. Kemény et al^[10] synthesized a new type of AlCoCrFeNi HEA film by electrochemical deposition method and discussed its corrosion behavior in 3.5wt% NaCl solution. It is found that the corrosion resistance of the HEA film is better than that of the copper substrate, and with increasing the Al content, the as-cast AlCoCrFeNi alloy is transformed from single-phase fcc structure to fcc and bcc mixture structure during the process, and ultimately to bcc structure when the alloy was prepared by vacuum arc casting method^[11]. The single-phase fcc solid solution normally contains <11at% Al, while the single-phase bcc solid solution contains at least 18.4at% Al in AlCoCrFeNi HEA system.

Molecular dynamics (MD) simulation can predict and analyze the microstructure and properties of HEAs. Lin et al^[12] studied the cascade process of atomic dissociation induced by

Received date: September 23, 2021

Foundation item: National Natural Science Foundation of China-Zhejiang Joint Fund for the Integration of Industrialization and Informatization (U1709210); Zhejiang Outstanding Talents Program (2018R51008); National Natural Science Foundation of China (51602087)

Corresponding author: Chen Wenhua, Ph. D., Professor, National and Local Joint Engineering Research Center of Reliability Analysis and Testing for Mechanical and Electrical Products, Zhejiang Sci-Tech University, Hangzhou 310018, P. R. China, Tel: 0086-571-86843367, E-mail: chenwh@zstu.edu.cn

Copyright © 2022, Northwest Institute for Nonferrous Metal Research. Published by Science Press. All rights reserved.

irradiation of NiCoCrFe HEA and pure Ni by MD method and the irradiation resistance mechanism of NiCoCrFe HEA was obtained through the comparative analysis. Choi et al.^[13] investigated the influence of each element on the solid solubility of the classical CoCrFeMnNi HEA with equiatomic ratio by MD simulation. It is found that the hysteresis diffusion effect is caused by the existence of numerous lattice holes with high migration barrier and stable energy in HEA, and the formation of micro-twinning at low temperature results from the more stable energy of hcp structure.

AlCoCrFeNi HEA has been widely studied due to its excellent properties with promising application potential^[14,15]. However, because of the complex multi-element components, it needs a lot of calculations to obtain an accurate potential function. In this research, the potential function in Ref. [16] was used to simulate the micro-crystal changes of Al_{0.1}CoCrFeNi single crystal HEA under axial tensile loading by MD method. Meanwhile, the effects of temperature and strain rate on the mechanical properties of the single crystal HEA were investigated, and the mechanism of crack propagation under tensile loading was analyzed by adding small surface cracks.

1 Simulation Model Construction

The Al_{0.1}CoCrFeNi HEA specimens for tensile tests were prepared^[17] into specific shape, as shown in Fig. 1a. The embedded atom method (EAM)^[18] and the potential function in Ref. [16] were used in this research. The Al_{0.1}CoCrFeNi has single-phase solid solution of fcc structure^[6,11]. The lattice constants of Co, Cr, Fe, and Ni are similar and the Al content is low, so the lattice constant of HEA was considered as 0.356 nm. The simulation model establishment was according to the following steps. The crystal structure was established based on fcc Fe element. Co, Cr, Ni, and Al atoms randomly replaced Fe atom sites in proportion to form Al_{0.1}CoCrFeNi single crystal HEA, and the interatomic interaction potential was defined for energy minimization. Then, the space rectangular coordinate system was established, and the model was stretched at strain rate of 10¹⁰ s⁻¹ along the y-axis after relaxation. The high strain rate of 10¹⁰ s⁻¹ is beneficial to the computational efficiency and short data analysis duration^[19-21]. Lammmps software was used to randomly replace the atoms on the perfect fcc structure to construct the fcc single crystal structure of Al, Ni, Co, Cr, and Fe elements with the molar ratio of 1: 10: 10: 10: 10. Periodic boundary conditions were employed in the simulation, and the model size was 20a×60a×20a (a is the lattice constant). There were 96 000 atoms in the whole model, and the time step of the whole simulation process was 1 fs.

Before the simulation of axial tensile loading, the whole system was minimized and relaxed under the isothermal isobaric ensemble. Thus, the whole simulation system reached the equilibrium state. During the loading process, the pressure was solely applied along y-axis. The quasi-static loading of the model was realized by regularly increasing the strain, and the position of each atom and the stress-strain values were

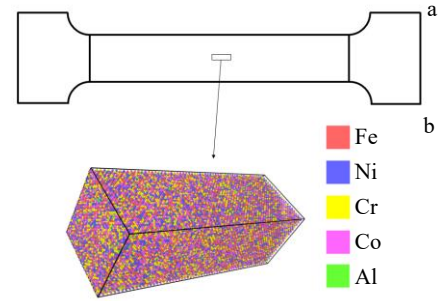


Fig.1 Schematic diagram of tensile specimen (a) and simulated atomic diagram (b) of Al_{0.1}CoCrFeNi single crystal HEAs

obtained.

2 Results and Discussion

2.1 Mechanical properties of Al_{0.1}CoCrFeNi single crystal HEA

Fig.2 shows the stress-strain curve of Al_{0.1}CoCrFeNi single crystal HEA under axial tensile loading at room temperature (300 K). It can be found that there are four stages: elastic deformation stage (E), yield deformation stage (A~C), strengthening stage (C~B), and plastic deformation stage (B~K).

The elastic deformation stage is the initial stress stage of solid materials, and the relationship between stress and strain is linear conforming to Hooke's law. In addition, Young's modulus can be obtained as 205 GPa, which is much higher than that of common single crystal metal or in the simulation. There is a long stage of hysteretic behavior, indicating that the alloy cannot be completely restored to its original state. The Young's modulus of Al_xCoCrFeNi HEAs with fcc structure is commonly 180~230 GPa^[3], inferring that the simulation results agree well with the experiment results.

With increasing the strain, the elastic deformation changes to plastic deformation, indicating the non-uniform plastic deformation stage. The maximum tensile strength is achieved in the uniform plastic deformation stage. In the non-uniform plastic deformation stage, the model deforms rapidly and

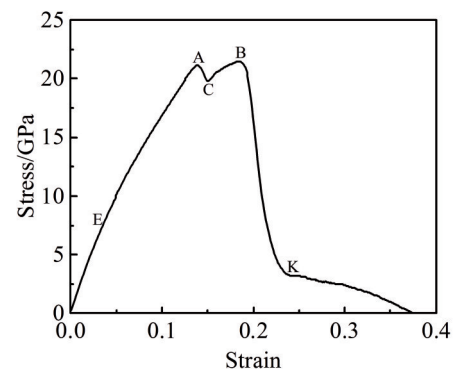


Fig.2 Stress-strain curve of Al_{0.1}CoCrFeNi single crystal HEA under axial tensile loading at room temperature

finally fractures. The yield strength, tensile strength, and calculated elongation^[21] is 21.1 GPa, 21.5 GPa, and 37.5%, respectively.

Fig. 3 reveals the crystal microstructure changes of $\text{Al}_{0.1}\text{CoCrFeNi}$ single crystal HEAs during tensile deformation by Ovito software and common neighbor analysis (CNA) method. Green, blue, red, and grayish white atoms represent the fcc, bcc, hcp, and disordered structure atoms, respectively.

Fig. 3a shows the atomic state at strain of 4.3%, and bcc structure atoms appear. Fig. 3b demonstrates the atomic state at strain of 13.9%, corresponding to the elastic phase and the end of the anelastic phase. Under this condition, the fcc, bcc, and disordered atoms account for 84.6%, 4.6%, and 10.8%, respectively. It is obvious that a large number of bcc atoms occur in the atomic model at strain of 15.0% (Fig. 3c). With increasing the strain from 13.9% to 15.0%, the formation of stacking faults and twinning causes the stress relaxation along the axial stress direction, and the stress suddenly drops in this stage. The decreasing rate is related to the formation rate of stacking faults and twinning. With increasing the strain from 15.0% to 18.4%, the number of bcc atoms slightly changes, while that of disordered atoms changes obviously. Meanwhile, the number of hcp atoms increases from basically zero to 8.4% in this stage. The increase in grain boundaries improves the strength and plastic deformation energy of the alloys, and therefore the stress is increased accordingly. Fig. 3e and 3f show the atomic states at strain of 23.5% and 29.9%, respectively. It is found that there are generous disordered atoms, the size of holes and other defects is increased, and the stress is decreased greatly with increasing the strain until fracture.

The stress after point C firstly increases and then decreases. This phenomenon may be attributed to the formation of three-dimensional stacking fault network, which hinders the dislocation movement and further provides a preferred position for the formation of hcp atoms, resulting in the strengthening stage^[22]. The effect of dislocation movement is different from that of the strain rate, and an obvious

strengthening process can be achieved in the appropriate strain rate range^[23].

2.2 Effect of strain rate on mechanical properties

MD models of $\text{Al}_{0.1}\text{CoCrFeNi}$ HEA were established under the simulation conditions of temperature of 300 K and the strain rates of 10^8 , 10^9 , 10^{10} , 10^{11} , and 10^{12} s^{-1} .

The stress-strain curves all show similar trends at different strain rates, as shown in Fig. 4. In the elastic deformation stage, the stress is linearly increased, and the elastic modulus is not affected by the strain rate. The strengthening stage is extremely short, and the stress decreases rapidly until fracture after entering into the yield stage.

Normally, the higher the strain rate, the bigger the radius of stress-strain curve around the peak value, therefore the longer the tensile process. It can be seen that the Young's modulus of $\text{Al}_{0.1}\text{CoCrFeNi}$ single crystal HEA is basically unchanged at different strain rates. As shown in Fig. 4, the yield strength is improved from 19.6 GPa to 33.6 GPa, i.e., it is increased by 71.4%, with increasing the strain rate from 10^8 s^{-1} to 10^{12} s^{-1} .

2.3 Effect of temperature on mechanical properties

The effect of temperature on the mechanical properties of $\text{Al}_{0.1}\text{CoCrFeNi}$ HEAs was investigated by increasing the simulation temperature from 100 K to 1000 K, as shown in Fig. 5 and Fig. 6. The general trends of stress-strain curves at different temperatures are consistent with those in Fig. 4. The stress is firstly increased linearly, slightly decreased, then increased again, and finally decreased until fracture. The simulation results show that the Young's modulus and strength of alloys are decreased with increasing the temperature in a certain range, which conforms to the traditional theory. With decreasing the simulation temperature, the maximum tensile strength is increased, and the elastic modulus rises slightly. The strain corresponding to the first peak stress increases, and the plasticity is improved simultaneously. When the average kinetic energy of atoms is small at low temperature, the plastic deformation occurs only when the tensile force is relatively large. With increasing the temperature, the average kinetic energy of atoms is increased greatly, and the force between

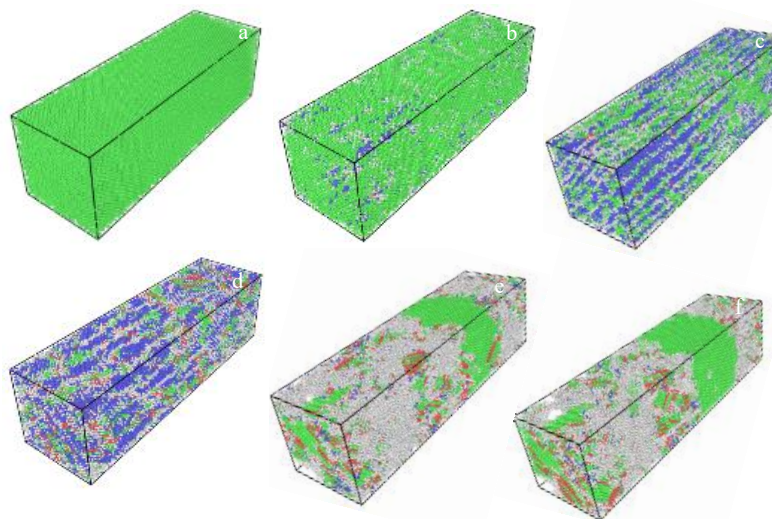


Fig.3 Microstructures of $\text{Al}_{0.1}\text{CoCrFeNi}$ single crystal HEAs at strain of 4.3% (a), 13.9% (b), 15.0% (c), 18.4% (d), 23.5% (e), and 29.9% (f)

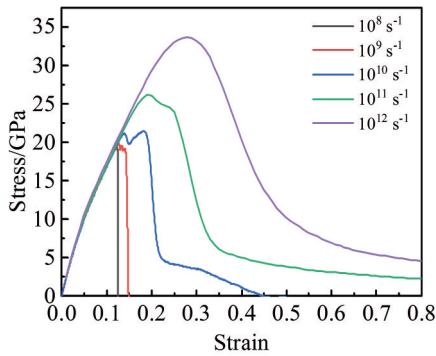


Fig.4 Stress-strain curves of $\text{Al}_{0.1}\text{CoCrFeNi}$ single crystal HEAs at different strain rates

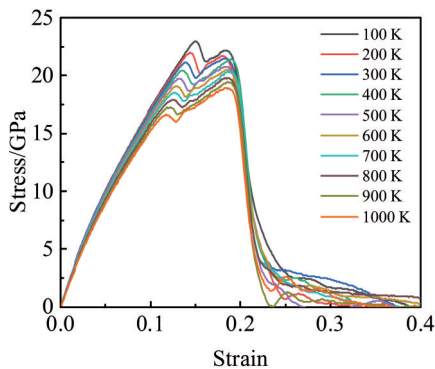


Fig.5 Stress-strain curves of $\text{Al}_{0.1}\text{CoCrFeNi}$ single crystal HEAs at different temperatures

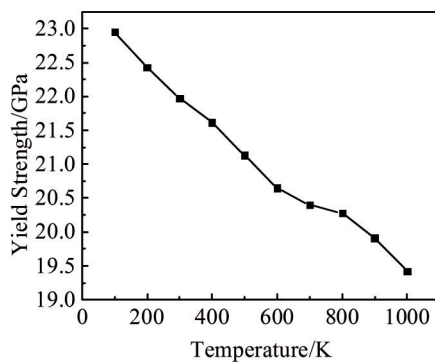


Fig.6 Yield strength of $\text{Al}_{0.1}\text{CoCrFeNi}$ single crystal HEAs at different temperatures

atoms is decreased with the addition of atomic spacing, which all result in the decreased Young's modulus, early plastic deformation, and the low ultimate tensile strength. The tensile simulation results at 300 and 100 K show good agreement with the experiment results of tensile properties of $\text{Al}_{0.3}\text{CoCrFeNi}$ HEA wire^[24]. The tensile strength and elongation are increased with reducing the temperature, and some nano-twins can be observed at low temperature.

2.4 Effect of surface crack on mechanical properties

In order to investigate the effect of surface cracks on the

mechanical properties of $\text{Al}_{0.1}\text{CoCrFeNi}$ single crystal HEAs, a crack was added on the model surface, as shown in Fig. 7. The size of the model cell is $20a \times 60a \times 20a$, and there is a small crack with a length of $20a$ on the surface. The simulated temperature is 300 K, and the relaxed configuration is uniformly stretched along the y -direction at the strain rate of 10^{10} s^{-1} .

According to Fig. 8, the surface crack leads to a significant decline in tensile strength and ductility of alloys. The crack does not affect the Young's modulus, but results in the formation of necking zone in tension, accelerating the fracture process. Therefore, the stress concentration occurs at the crack tip and the slip dislocation is formed.

As shown in Fig. 9a, the line defect is formed on the symmetrical surface of the crack due to the tensile loading. A linear defect also appears on the symmetrical surface of initial crack due to the tensile loading, and the necking zone is formed with increasing the strain. The hcp atoms appear when the strain is 7.4%. Before that, the atoms are all fcc atoms. When the strain is 9.9%, there are only a few bcc atoms. The stress concentration at the crack tip is notable on the opposite side of the initial crack, and the atoms near the defects are staggered to form the slip dislocation.

The tensile strength reaches the maximum when the strain is 12.4%, and abundant slip dislocations are formed with the development of $1/6\langle 110 \rangle$ Schottky dislocation fragments in

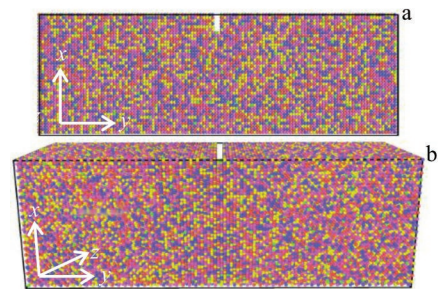


Fig.7 Simulated 2D (a) and 3D (b) atomic diagrams of $\text{Al}_{0.1}\text{CoCrFeNi}$ single crystal HEAs with a surface crack

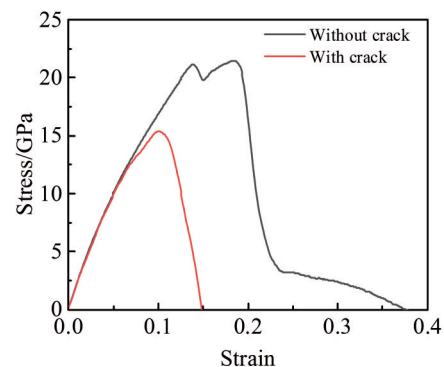


Fig.8 Stress-strain curves of $\text{Al}_{0.1}\text{CoCrFeNi}$ single crystal HEAs with and without a surface crack at temperature of 300 K and strain rate of 10^{10} s^{-1}

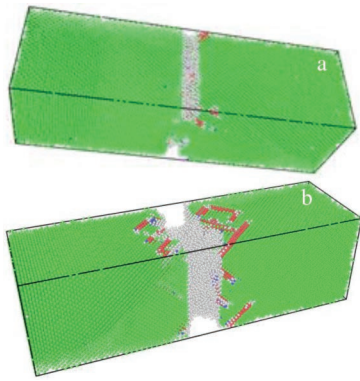


Fig.9 Microstructures of $\text{Al}_{0.1}\text{CoCrFeNi}$ single crystal HEAs with surface crack at strain of 9.9% (a) and 12.4% (b)

the $\text{Al}_{0.1}\text{CoCrFeNi}$ single crystal HEAs with a surface crack. The stress is decreased rapidly with the deformation further proceeding, and the necking area becomes larger and larger until fracture, as shown in Fig.9b.

3 Conclusions

1) The $\text{Al}_{0.1}\text{CoCrFeNi}$ single crystal high entropy alloy (HEA) under axial tensile loading at room temperature undergoes four stages: elastic deformation stage, yield deformation stage, strengthening stage, and plastic deformation stage before fracture. The Young's modulus of nanocrystalline can reach 205 GPa, and the tensile stress decreases and then increases in a short time after reaching the yield strength, because of the formation of massive body-centered cubic (bcc) atoms.

2) The stress-strain curves of $\text{Al}_{0.1}\text{CoCrFeNi}$ single crystal HEAs are similar at different strain rates within a certain range. The elastic deformation stage shows an approximately linear rise in stress. The strengthening stages are quite short after entering into the yield deformation stage, and the stress decreases rapidly until fracture. The higher the strain rate, the longer the tensile process, which is related to the growth of dislocation density and tensile resistance with increasing the strain rate.

3) With increasing the temperature, the stress is firstly increased and then decreased rapidly. The elastic deformation stage is very short and the maximum tensile strength is high. The decrease in simulation temperature can increase the yield strength, maximum tensile strength, plasticity, and Young's modulus, because the dislocation motion resistance is increased and the atomic thermal activation ability is decreased.

4) The surface crack does not affect the elastic modulus and leads to the formation of necking zone in the $\text{Al}_{0.1}\text{CoCrFeNi}$ single crystal HEA. It is worth mentioning that the stress concentration at the crack tip results in the formation of slip

dislocation, which accelerates the fracture process.

References

- 1 Yeh J W, Chen S K, Lin S J et al. *Advanced Engineering Materials*[J], 2004, 6(5): 299
- 2 Zhang Y, Zuo T T, Tang Z et al. *Progress in Materials Science* [J], 2014, 61: 1
- 3 Li W D, X D, Li D Y et al. *Progress in Materials Science*[J], 2021, 118: 100 777
- 4 Chang Haitao, Huo Xiaofeng, Li Wanpeng et al. *Rare Metal Materials and Engineering*[J], 2020, 49(10): 3663 (in Chinese)
- 5 Yang T H, Cai B, Shi Y J et al. *Micron*[J], 2021, 147: 103 082
- 6 Fan Q K, Chen C, Fan C L et al. *Surface and Coatings Technology*[J], 2021, 418: 127 242
- 7 Maresca F, Curtin W A. *Acta Materialia*[J], 2020, 182: 235
- 8 Vaidya M, Sen S, Zhang X et al. *Acta Materialia*[J], 2020, 196: 220
- 9 Rogal L, Szklarz Z, Bobrowski P et al. *Metals and Materials International*[J], 2019, 25(4): 930
- 10 Kemény D M, Miskolczi P N, Fazakas É. *Materials Today: Proceedings*[J], 2021, 45(5): 4250
- 11 Wang W R, Wang W L, Wang S C et al. *Intermetallics*[J], 2012, 26: 44
- 12 Lin Y P, Yang T F, Lang L et al. *Acta Materialia*[J], 2020, 196: 133
- 13 Choi W M, Jo Y H, Sohn S S et al. *Computational Materials*[J], 2018, 4(1): 1
- 14 Yang H X, Li J S, Guo T et al. *Rare Metals*[J], 2019, 39(2): 156
- 15 Yang H X, Li J S, Pan X Y et al. *Journal of Materials Science and Technology*[J], 2021, 72: 1
- 16 Farkas D, Caro A. *Journal of Materials Research*[J], 2020, 35(22): 3031
- 17 Ma N, Liu S F, Liu W et al. *Frontiers in Bioengineering and Biotechnology*[J], 2020, 8: 603 522
- 18 Baskes M I, Daw M S, Foiles S M. *MRS Symposia Proceedings* [J], 1988, 141: 31
- 19 Liu Xiaobo, Xiong Zhen, Fang Zhou et al. *Rare Metal Materials and Engineering*[J], 2019, 48(9): 2745
- 20 Li Jian, Guo Xiaoxuan, Ma Shengguo et al. *Chinese Journal of High Pressure Physics*[J], 2020, 34(1): 35 (in Chinese)
- 21 Cao Hui, Rui Zhiyuan, Feng Ruicheng et al. *Rare Metal Materials and Engineering*[J], 2019, 48(4): 1102
- 22 Chen S, Oh H S, Gludovatz B et al. *Nature Communication*[J], 2020, 11(1): 826
- 23 Fan H D, Wang Q Y, El-Awady J A et al. *Nature Communication* [J], 2021, 12(1): 1845
- 24 Li D Y, Li C X, Feng T et al. *Acta Materialia*[J], 2017, 123: 285

Al_{0.1}CoCrFeNi高熵合金力学性能分子动力学研究

郑伟¹, 韩俊昭¹, 段星², 陈文华¹

(1. 浙江理工大学 机电产品可靠性分析与测试国家地方联合工程研究中心, 浙江 杭州 310018)

(2. 杭州电子科技大学 材料与环境工程学院, 浙江 杭州 310018)

摘要: 通过分子动力学方法研究了Al_{0.1}CoCrFeNi单晶高熵合金在室温(300 K)下沿轴向拉伸后的组织和力学性能变化。通过改变模拟应变速率和温度, 分析了单晶高熵合金的拉伸性能; 通过模拟室温拉伸实验, 研究了含表面小裂纹单晶的显微组织和拉伸性能。结果表明, 当应变速率在一定范围内时, 抗拉伸强度随应变速率增大而增大; 当应变速率为10¹⁰ s⁻¹时, 杨氏模量和抗拉伸强度随温度降低而增大。表面有贯穿小裂纹的单晶高熵合金在拉伸一段时间后出现颈缩现象, 随着大量滑移位错的快速发展, 裂纹尖端出现应力集中, 导致快速断裂。

关键词: 高熵合金; 分子动力学; 拉伸性能; 裂纹

作者简介: 郑伟, 男, 1987年生, 博士生, 浙江理工大学机电产品可靠性分析与测试国家地方联合工程研究中心, 浙江 杭州 310018, E-mail: 202010601024@mails.zstu.edu.cn